PHOTONICS Research

Immensely enhanced color-adjustable upconversion fluorescence in electron donor-acceptor exciplex chromophores doped with fluorescent emitters

ZHEN CHEN,[1] QIAN ZHOU,[1] HUITIAN DU,[1] YUAN YU,[1] CHUANG ZHANG,[2] SHENGHAO HAN,[1] AND ZHIYONG PANG[1,*]

[1]School of Microelectronics, State Key Laboratory of Crystal Materials, Shandong University, Jinan 250100, China
[2]Institute of Chemistry, Chinese Academy of Sciences, Beijing 100190, China
*Corresponding author: pang@sdu.edu.cn

Received 19 October 2020; revised 9 March 2021; accepted 9 March 2021; posted 9 March 2021 (Doc. ID 412860); published 30 April 2021

Two-photon excited fluorescence materials usually suffer from inefficient two-photon absorption (TPA) and nonradiative excited states. Here, upconversion fluorescence in an electron donor-acceptor (DA) exciplex doped with fluorescent emitters are systematically investigated. It has been found that the undoped DA exciplex exhibits enhancements of ∼129% and ∼365% in upconversion fluorescence compared to donor- and acceptor-only systems, respectively. Interestingly, photoluminescence quantum yields (PLQYs) up to ∼98.65% were measured and immensely enhanced upconversion fluorescence was observed after doping various fluorescent emitters into the DA exciplex. Our results reveal the existence of two-photon excited energy harvesting in a thermally activated delayed fluorescence (TADF) DA exciplex doped with fluorescent emitters, via reverse intersystem crossing followed by rapid Förster resonance energy transfer. Moreover, the additional gain mechanism related to intermolecular CT interaction that occurs at the TPA stage is found in the TADF DA exciplex system.

https://doi.org/10.1364/PRJ.412860

1. INTRODUCTION

In last few decades, two-photon excited fluorescence (TPEF) has attracted increasing research interest for its growing list of applications that include two-photon imaging. Researchers are attracted by its tremendous advantages: high three-dimensional resolution, strong penetrability to biological tissues, and restricted photobleaching and phototoxicity [1–3]. Technically, TPEF materials with excellent two-photon absorption and light emission properties are essential and highly desired for two-photon imaging applications. Unfortunately, two-photon excitation is intrinsically much less efficient than a one-photon process [4–6]. To solve this problem, great efforts have been devoted to the design and discovery of dye molecules with large two-photon absorption cross-sections; particularly, complicated molecular architectures in view of the relationship between the two-photon absorption cross-section and the dipole moment [7–9]. However, this often results in inefficient radiative excited states due to the fast "internal conversion" mechanism, together with a great increase in the cost of commercial products caused by increased synthetic steps [10,11]. As a result, developing a facile, efficient strategy to obtain low-cost, highly efficient TPEF dyes with enhanced performance remains a challenge [12–14].

Besides two-photon absorption, there is another key parameter that is crucial for TPEF dyes: the fluorescence quantum efficiency. The fluorescence quantum efficiencies of organic chromophores are greatly restricted by the nonradiative excited states [15,16]. Recently, great advances have been made in the new emerging field of thermally activated delayed fluorescence (TADF) materials by minimizing the energy splitting, ΔE_{ST}, between singlet and triplet states to efficiently facilitate the reverse intersystem crossing (RISC) process from triplet to singlet states [17–19]. This energy harvesting mechanism is ideal for TPEF dyes, although very few intrinsic (single-component) TADF molecules have been discovered to show two-photon absorption (TPA) properties. The energy harvesting becomes even more efficient in extrinsic TADF materials in which RISC occurs in exciplexes (EX) of designed electron donor (D) and acceptor (A) [20–22]. In particular, the light emission can be further enhanced by adding a tiny amount of fluorescent dopant into TADF hosts [23,24]. The rapid Förster resonance energy transfer (FRET) from the singlet EX states to the lowest

singlet states of the fluorescent emitter leads to more intense fluorescent emission [25,26]. Nevertheless, possible TPEF processes have not been explored in these systems, which may provide a new avenue for a new material design strategy for highly efficient TPEF materials.

In this work, we observed and studied the TPEF in thin films of TADF DA exciplex and exciplex doped with a fluorescent emitter. The host blend is composed of 1,1-bis[(di-4-tolylamino)phenyl]cyclohexane (TAPC) as the donor and tris-[3-(3-pyridyl)mesityl]borane (3TPYMB) as the acceptor. The fluorescent emitters used in this work are 9,10-bis[N,N-di-(ptolyl)-amino]anthracene (TTPA) and 4-(dicyanomethylene)-2-methyl-6-(p-dimethylaminostyryl)-4H-pyran (DCM). The upconversion fluorescence is achieved upon 760 nm excitation corresponding to exciplex emissions in an undoped DA blend. The enhancements of upconversion fluorescence from the DA blend are ∼129% and ∼365% compared to donor-/acceptor-only systems, respectively. Most interestingly, we found that the upconversion fluorescence intensities of the exciplex samples increased dramatically after doping a tiny amount of the fluorescent emitter. The immensely enhanced upconversion fluorescence in the doped DA exciplex is due to the existence of RISC followed by rapid FRET processes, which facilitate the energy harvesting processes and lead to more efficient upconversion fluorescence. Notably, these specific DA blends with the addition of fluorescent emitters have the advantages of two-photon absorption and a high quantum yield, so that they may have broad application prospects in the field of two-photon fluorescence imaging.

2. EXPERIMENTAL SECTION

Materials preparation: The thin films of pristine TAPC [99.5%, Luminescence Technology Corp. (Lumtec), New Taipei City], 3TPYMB (99%, Lumtec), TAPC:3TPYMB blend, TTPA-doped TAPC:3TPYMB blends, and DCM-doped TAPC:3TPYMB blends were prepared using a drop-casting method. The donor molecule TAPC and acceptor molecule 3TPYMB, the green fluorescent emitter molecule TTPA (99%, Lumtec) and the orange fluorescent emitter molecule DCM (99%, Lumtec) were dissolved in tetrahydrofuran solvent at a concentration of 20 mg/mL. Subsequently, the solution was stirred overnight prior to film preparation. Quartz substrates were selected for optical property measurements. A tetrahydrofuran solution of each emitter dopant (10^{-5} mol/L) was used for the measurement of absorption.

Measurements: The absorption spectra were measured using a UV-vis spectrophotometer (TU-1901, Beijing Purkinje General Instrument Co., Ltd., Beijing). A tungsten lamp and a deuterium lamp are used as the light sources in the visible and ultraviolet ranges, respectively, and we set it at 375 nm to change the lamp. The photoluminescence spectra were measured using a fluorescence spectrophotometer (F-4500, Hitachi, Ltd., Tokyo). The light source is a xenon lamp, and the excitation wavelength is set to 330 nm. Transient photoluminescence (PL) decay characteristics were measured with a fluorescence spectrometer (FLS920, Edinburgh Instruments Ltd., Livingston, Scotland) using an EPLED-280 laser (excitation wavelength of 280.6 nm, pulse width of 945.1 ps, and bandwidth of 11.0 nm). Photoluminescence quantum yields (PLQYs) were measured by an absolute PL quantum yield measurement system (FLS920, Edinburgh Instruments) with an integrating sphere under an excitation wavelength of 330 nm (xenon lamp). For the measurement of two-photon induced fluorescence spectrum, a Ti:sapphire femtosecond pulse amplification system (Legend Elite series, pulse width of 25 fs, repetition rate of 1000 Hz, Coherent Inc., Santa Clara, CA) was used to excite the samples. The upconverted emission was measured using a monochromator (Omni-λ300, Zolix Instruments Co., Ltd., Beijing) together with a PMTH-S1C1-CR131 photomultiplier tube.

3. RESULTS

A. TPEF Studies of DA Exciplex

Molecular structures of the donor TAPC and acceptor 3TPYMB are shown in Fig. 1(a). For TAPC, two electron-rich tri(p-tolyl) amine groups are chemically bridged by a cyclohexane ring formed by a D-π-D structure [27,28]; for 3TPYMB, a starburst structure is formed by an electron-deficient trimesitylborane core and pyridyl branches [29,30]. These TPA-active molecular structures indicate that an effective TPA may exist in these two components [31–33]. Figure 1(b) shows the energy-level alignment of TAPC and 3TPYMB, in which the highest occupied molecular orbital (HOMO) and the lowest unoccupied molecular orbital (LUMO) energies are taken from literature [34–36]. The large energy offsets between HOMO (1.2 eV) and LUMO (1.3 eV) enable an efficient charge separation and the following exciplex formation processes after being excited [37].

Figure 1(c) shows the normalized room temperature PL and optical absorption spectra of films of the pristine TAPC and 3TPYMB, and the TAPC:3TPYMB (1:1) DA blend. The PL emission spectra of TAPC and 3TPYMB peak at 384 nm and 385 nm, respectively; whereas the PL emission spectrum from the blend shows a significantly red-shifted single peak at ≈460 nm. This indicates near 100% formation of photoexcited DA exciplexes in the blend [38,39]. Based on a modified Rehm–Weller equation: $-\Delta G_{CS} = E_{exciton} - E_{exciplex}$ [40], a suitable value (≈0.6 eV) of the driving force $-\Delta G_{CS}$ for exciplex formation was estimated [41,42]. This may explain the observed PL emission spectrum from the DA blend. In comparison, the optical absorption spectrum from the blend shows contributions entirely from D and A molecules. No obvious optical absorption in the range of the DA exciplex, which is significantly red-shifted compared to that of excitons of D or A, can be observed. This reveals that the exciplexes in the blend originate from a photoexcited D and/or A instead of optical transitions from the ground states to the EX states [43]. We note that this is different with another DA-type material named ground state charge-transfer (CT) cocrystals, in which the optical absorption occurs via transitions from the ground states to the CT exciton states instead of the exciton states of D or A, leading to significantly red-shifted optical absorption edges in their optical absorption spectra [44]. Accordingly, this difference in the optical absorption mechanism may bring about a different design strategy for the TPEF material. For ground state CT cocrystals, TPEF materials can be designed based on TPA-free components in view of

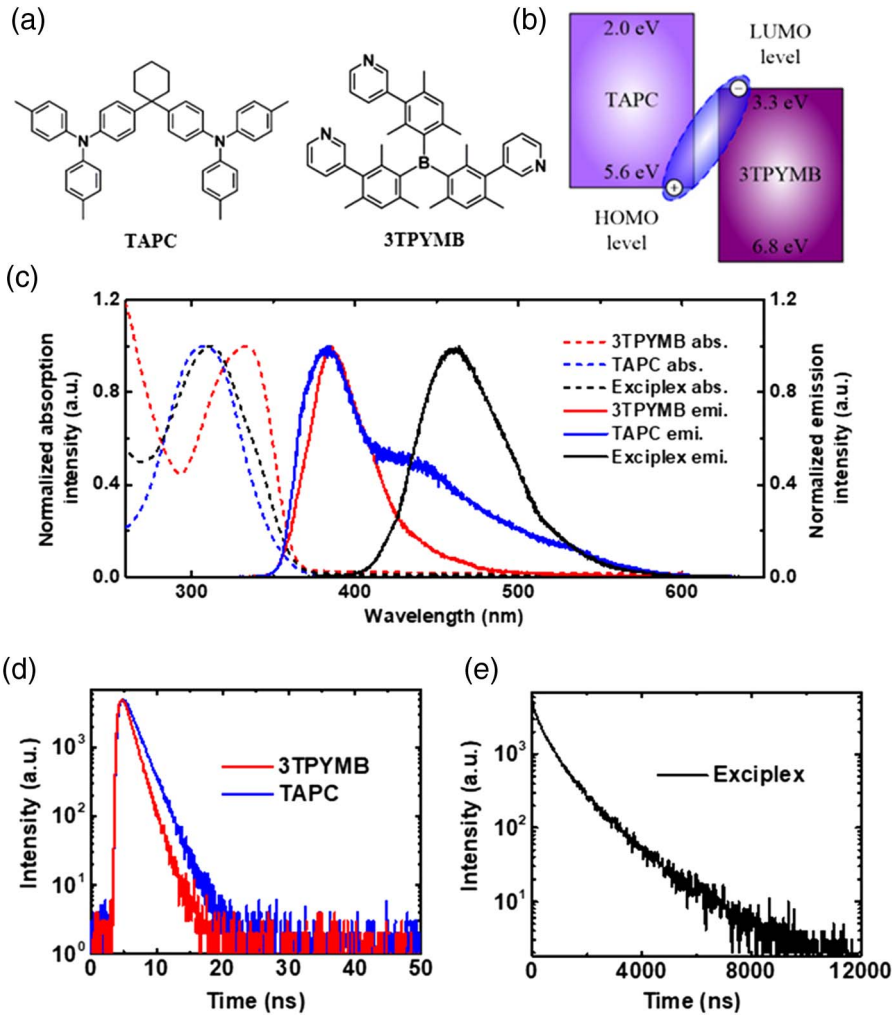

Fig. 1. (a) Molecular structures of the donor TAPC and the acceptor 3TPYMB. (b) Energy diagram of TAPC and 3TPYMB, and scheme of exciplex formation. (c) Normalized optical absorption spectra and PL spectra of TAPC, 3TPYMB, and TAPC:3TPYMB blend (1:1). (d) Room temperature photoluminescence decay curve of TAPC and 3TPYMB. (e) Room temperature PL decay curve of TAPC:3TPYMB blend (1:1).

the relationship between TPA and intermolecular CT interactions [45]; however, TPA components are necessary for the design of exciplex-based TPEF material since the photons in the exciplex blend are absorbed by D or A components.

The room temperature PL decay curves of films of the pristine TAPC and 3TPYMB, and the TAPC:3TPYMB (1:1) DA blend measured at their PL emission peaks are shown in Figs. 1(d) and 1(e). The short PL lifetimes ($\tau = 1.9$ ns and 1.4 ns for TAPC and 3TPYMB, respectively) and monoexponential decay of PL intensities of D and A indicate fluorescent emission from singlet excitons [46]. However, the transient PL decay curve of the blend shows an extremely long lifetime that contains double exponential components, $\tau =$ 251.1 ns and 950.4 ns with proportions of 53% and 47%, respectively. The prolonged fluorescence lifetimes of the blend reveal effective TADF RISC processes from the triplet states (^{3}EX) to the singlet states of DA exciplex (^{1}EX) in the blend [47].

Figures 2(a) and 2(b) illustrate one-/two-photon excited fluorescence processes in conventional exciton-type molecules and TADF exciplex-type materials, respectively. For conventional exciton-type molecules, for example, pristine D molecules, the initial one-/two-photon excitation decay occurs very fast from the excited donor states to the singlet exciton (^{1}D), followed by fluorescent emission. It is tempting to assume that all of the photo-generated ^{1}D produces fluorescence emission; under this condition, the PLQYs of exciton-type molecules would be 100%. However, energy loss mechanisms such as the intersystem crossing (ISC) from ^{1}D to the triplet exciton (^{3}D) is quite feasible since the energy level of ^{3}D is much lower than that of ^{1}D [48]. This leads to substantial population of nonradiative ^{3}D that is generated in parallel with the fluorescence emission process of ^{1}D. This may explain the reported low PLQY (much lower than 100%) of most molecules. For TADF exciplex-type materials, however, the ΔE_{ST} between ^{1}EX and ^{3}EX is rather small, giving rise to efficient RISC from ^{3}EX to ^{1}EX and thus an increased PLQY of 5%–100% [49]. This provides a possibility to achieve enhanced TPEF in TADF exciplex-type materials.

To explore the nonlinear optical properties of TADF exciplex-type material, long-wavelength-excited fluorescence measurements of the DA blend (1:1) were investigated using a near-infrared femtosecond laser. As shown in Fig. 3(a), the

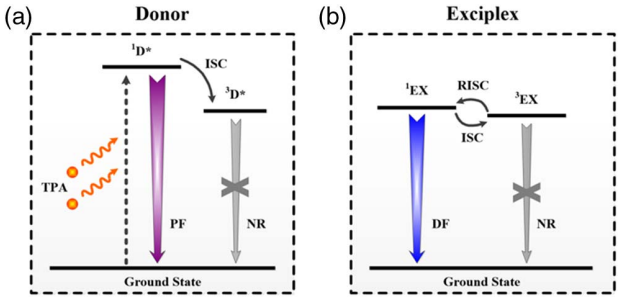

Fig. 2. (a) Schematic diagram of the one-/two-photon excited fluorescence process in conventional exciton-type molecules. (b) Schematic of the fluorescence enhancement from the TADF process. TPA, two-photon absorption; ^{1}D*, singlet state of donor; ^{1}EX, singlet states of DA exciplex; ^{3}EX, triplet states of DA exciplex; ISC, intersystem crossing; RISC, reverse intersystem crossing; PF, prompt fluorescence; DF, delayed fluorescence; and NR: nonradiative transition.

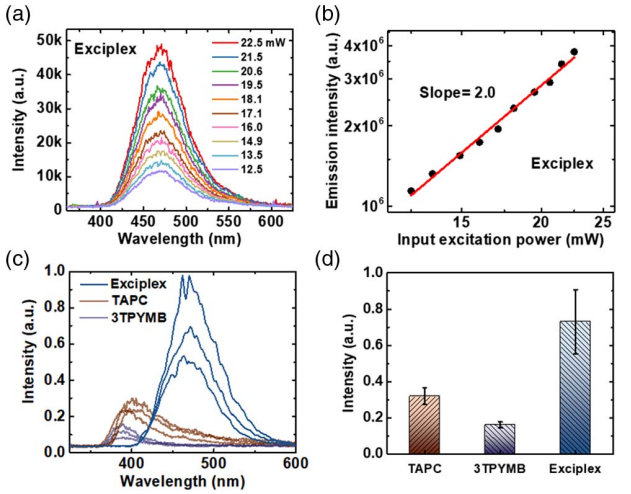

Fig. 3. (a) Upconversion PL spectra of TAPC:3TPYMB blend (1:1) under 760 nm excitation at different powers. (b) Log-log plot of the integrated area of PL spectra versus the power intensities of input laser by using the data of (a). (c) Two-photon excited fluorescence spectra of TAPC, 3TPYMB, and TAPC:3TPYMB blend (1:1) under 760 nm excitation at the same condition. Three spectra were measured in different areas for each sample. (d) Comparison of average integrated area of PL spectra using the corresponding data of (c).

DA blend shows a strong blue emission with a peak at ≈470 nm upon 760 nm excitation, revealing an efficient upconversion process in the blend. The upconversion PL spectra of the blend exhibit almost the same shape and wavelength distribution as that of downconversion PL measurement [Fig. 1(c)], indicating that the upconversion fluorescence originates from radiative transition from the EX states also to the ground states [45]. In addition, the intensities of the upconversion fluorescence from the DA blend increase gradually with the power of the excitation laser. From the log–log plot of the integrated area of emission spectra versus the power intensity of input laser [Fig. 3(b)], a slope of 2.0 is obtained. This implies that the upconversion fluorescence stems from a two-photon absorption process [50]. We have also measured the long-wavelength-excited fluorescence properties of pristine D and A, and the results exhibit that both D and A show TPEF upon 760 nm excitation by using a near-infrared femtosecond laser operating at 1 kHz. Combined with the optical absorption and PL analysis mentioned above, we speculate that the TPEF in the film of TADF DA blend originates from a two-photon-excited exciplex formation process that is composed of a TPA process of D and/or A and a following exciplex formation process. It is found that the intermolecular CT interactions between two-photon excited donors and ground state acceptors (or vice versa) give rise to a near 100% formation of DA exciplex under the influence of the driving force $-\Delta G_{CS}$ because the TPEF spectra of the DA blend only show exciplex emission bands, and no obvious fluorescence contributions from the D or A molecules can be observed.

Considering the triplet harvesting mechanism existing in the TADF exciplex, an enhanced TPEF from exciplex can be theoretically expected [51]. We thus investigate the TPEF properties of pristine D, A, and DA blend under the same conditions. As shown in Fig. 3(c), all the TPEF spectra of the DA blends show a giant enhancement compared to that of pristine D and A, confirming experimentally the existence of the TPEF enhancement mechanism in exciplex systems. By integrating and averaging the intensities of TPEF bands of D, A, and DA blend [Fig. 3(d)], average enhancements of ∼129% and ∼365% are calculated for D and A, respectively. It is reasonably deduced that RISC processes from the triplet states (^{3}EX) to the singlet states of DA exciplex (^{1}EX) in the blend enhanced the TPEF. We also measured the PLQY of the pristine D, A, and DA blend, and the results show that the PLQY of the DA blend (7.40%) is higher than that of the pristine D (6.45%) and A (4.01%). We note that the obtained TPEF enhancement is larger than that of PLQY, indicating there may exist another possible enhancement mechanism for TPEF in the exciplex DA blend. We speculate that the intermolecular CT interaction may be responsible for the enhancement of TPEF, because it has been found to facilitate two-photon absorption [52], and it exists in the excited state of the DA blend and gives rise to the formation of the exciplex [53].

B. TPEF Studies of DA Exciplex Doped with Fluorescent Emitters

Figure 4(a) shows the molecular structures of two fluorescent emitters: TTPA and DCM. In the host-dopant system, an effective FRET process occurs only when the absorption peak of the dopant overlaps with the emission band of the host [54]. To verify the suitability of the fluorescent emitters, we selected the normalized optical absorption for the TAPC:3TPYMB exciplex system, and the PL spectra of TTPA and DCM were measured at room temperature and shown in Fig. 4(b). As a reference, the normalized PL emission band of the TAPC:3TPYMB (1:1) DA blend host is also provided as a dark area. The PL spectra of TTPA and DCM each show a single emission band with peaks at 532 nm and 570 nm, respectively. We note that the absorption bands of both TTPA and DCM overlap perfectly with the PL emission band from the exciplexes in the blend host, indicating that an effective FRET process may occur from the

singlet state of the exciplex (^{1}EX) to the singlet state of the fluorescent emitter (^{1}EM).

Figures 4(c) and 4(d) show the normalized PL spectra of the DA blend hosts doped with various concentrations of TTPA and DCM fluorescent emitters, respectively. It can be found that the emission intensities from the fluorescent emitters exceed that of the DA blend host at a concentration of 0.2% for both TTPA and DCM. This reveals that the FRET process is very efficient in these systems. As the concentrations of the fluorescent dopants increase to 0.5%–1%, most of the fluorescence results from the emitter. This may partially explain why most of the reported concentrations of fluorescent emitters in the TADF-based organic light-emitting diodes (OLEDs) are 1% [24,25,55]. As the concentration of the dopants increased to 2%, only fluorescence contributed by fluorescence emitters was observed. Therefore, we use 2% as the dopant concentration to study the TPEF mechanisms of the DA exciplex doped with fluorescence emitters in this work.

Figure 4(e) shows the room temperature PL decay curves of TTPA- and DCM-doped DA blends measured at their PL emission peaks. Both TTPA- and DCM-doped DA blends show double lifetime components. For the TTPA-doped DA blend, $\tau = 37.4$ ns and 245.3 ns are obtained; for DCM-doped samples, the lifetime components are $\tau = 4.3$ ns and 19.8 ns, respectively. We note that these values are much shorter than that of undoped DA blends (251.1 ns and 950.4 ns), indicating an efficient rapid FRET process from the singlet ^{1}EX state of the exciplex host to the singlet ^{1}EM state of the dopant emitter [56]. It is also found that the proportions of prompt components are 97.4% and 83.3% for TTPA- and DCM-doped DA blends, respectively. We note that these values are much higher than that of the undoped DA blend discussed above, revealing that the majority of singlet exciplex states of the host directly transfer to the singlet exciton states of the dopant via FRET and then give rise to prompt fluorescence [57]. Thus, the energy loss during the mutual conversion between the singlet state and the triplet state of the exciplex may be weakened and the fluorescence quantum efficiency can therefore be further increased. We thus expect that enhanced TPEF may also be achieved in a TADF DA blend doped with fluorescent emitters, because a similar FRET process may occur on the two-photon excited exciplexes. In addition, we prepared organic light-emitting devices based on exciplex doped with 2% TTPA and measured the electroluminescence spectrum [Fig. 4(f)]. The devices have obvious green light emissions with an emission peak at 528 nm. We believe that this fluorescent doped exciplex system with ultra-high PLQYs may also have broad application prospects in the field of light-emitting devices.

Figures 5(a) and 5(b) show the power-dependent long-wavelength-excited fluorescence spectra of TAPC:3TPYMB (1:1) blends doped with 2% (mass fraction) TTPA and 2% (mass fraction) DCM, respectively. Under 760 nm excitation, the TTPA-doped DA blends show strong green emission with their peaks at ≈555 nm; the orange emission bands that peak at ≈625 nm, however, are observed for the DCM-doped DA

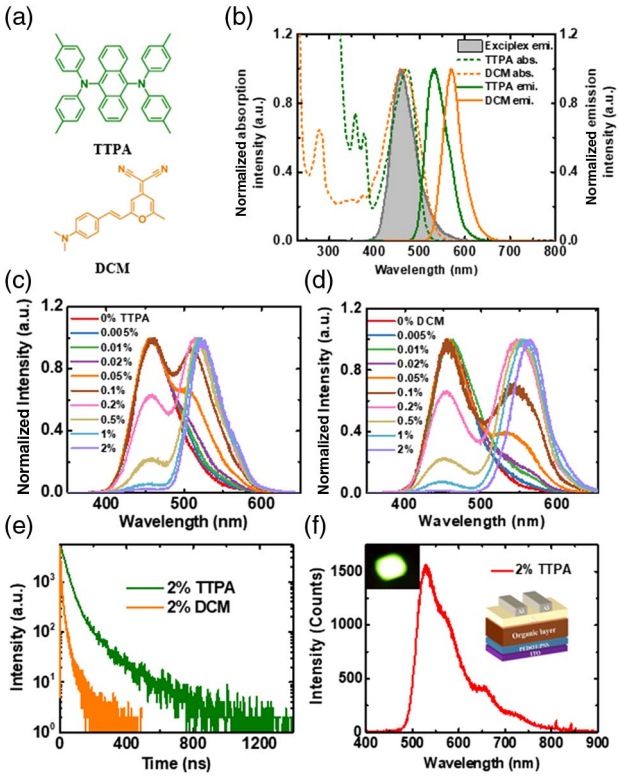

Fig. 4. (a) Molecular structures of emitter dopants TTPA and DCM. (b) Normalized room temperature optical absorption and PL spectra of emitter dopants TTPA and DCM. The dark area shows the normalized PL emission band of the TAPC:3TPYMB (1:1) DA blend host. (c) Steady state PL spectra of TAPC:3TPYMB (1:1) blends doped with a TTPA emitter dopant at various concentrations. (d) Steady-state PL spectra of TAPC:3TPYMB (1:1) blends doped with DCM emitter dopant at various concentrations. (e) PL decay curves of 2% DCM- and TTPA-doped TAPC:3TPYMB (1:1) blends. (f) Electroluminescence spectrum of organic light-emitting devices based on exciplex doped with 2% TTPA. (Inset: device structure and photo image of the emission.)

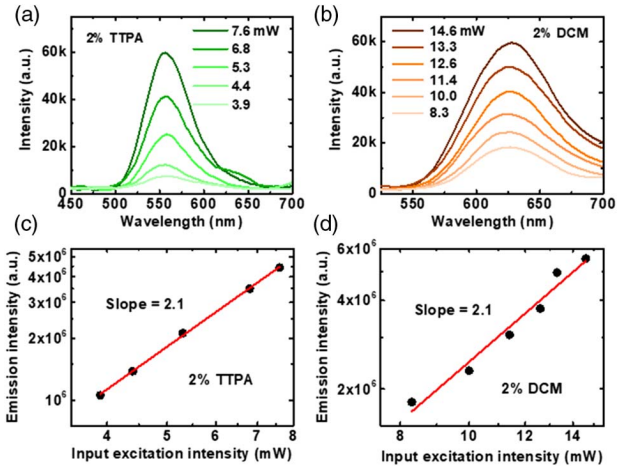

Fig. 5. Power-dependent, long-wavelength-excited fluorescence spectra of TAPC:3TPYMB (1:1) blends doped with (a) 2% TTPA and (b) 2% DCM. (c) Log–log plot of the integrated area of PL spectra versus the power intensity of input laser by using the data of (a). (d) Log–log plot of the integrated area of PL spectra versus the power intensity of input laser by using the data of (b).

blends. This reveals the efficient upconversion processes in these films. Moreover, the upconversion PL spectra of the emitter-doped blends exhibit similar emission bands to that of the downconversion PL spectra, indicating that the upconversion and downconversion emission may originate from the same excited state [58]. As shown in Figs. 5(c) and 5(d), the slopes of the log–log plot of the integrated area of the emission spectra versus the input power intensities for TTPA- and DCM-doped DA blends are both calculated to be ~2.1, implying that the observed upconversion fluorescence from these samples stems from a two-photon absorption process [59].

Figure 6(a) shows the normalized long-wavelength-excited fluorescence spectra of the pristine A, undoped DA blend, TTPA-doped DA blend, and DCM-doped DA blend. Different emission colors of purple, blue, green, and orange were obtained by adjusting the material components. This is technically useful for many TPEF applications. We note that this method is theoretically extensible. More colors can be potentially obtained in this blend by adjusting the dopants, or in other TADF DA blend systems, through reasonable material design. In the case of the existence of an effective FRET process from the singlet exciplex state of the host to the singlet state of the fluorescent emitter, the color of TPEF can be theoretically adjusted by doping a tiny amount of fluorescent emitter.

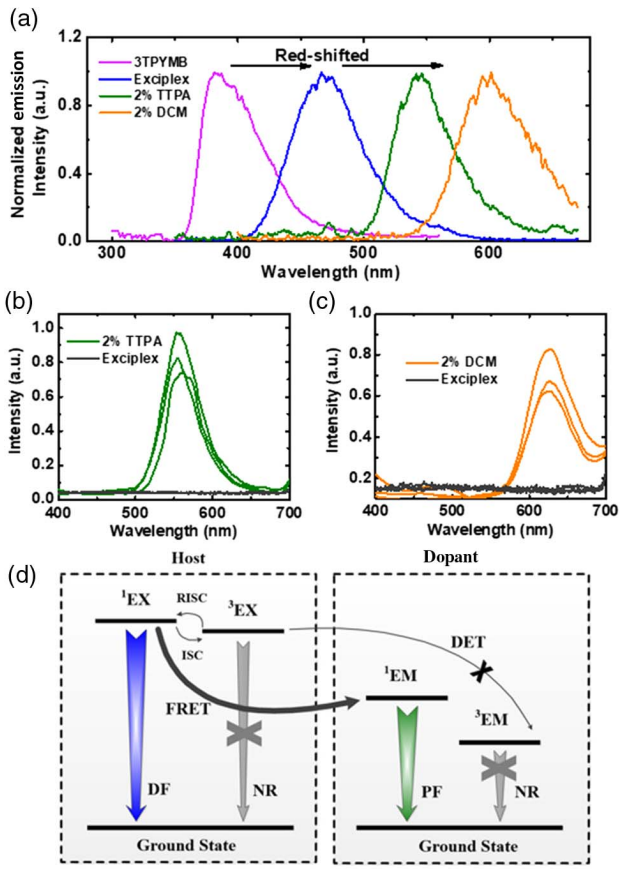

Fig. 6. (a) Normalized long-wavelength-excited fluorescence spectra of pristine A, undoped DA blend, TTPA-doped DA blend, and DCM-doped DA blend. (b) Two-photon excited fluorescence spectra of undoped- and 2% TTPA-doped TAPC:3TPYMB blend (1:1) measured at the same condition. (Three curves with the same color indicate that the same sample has been measured three times.) (c) Two-photon excited fluorescence spectra of undoped- and 2% DCM-doped TAPC:3TPYMB blend (1:1) measured at the same condition. For (b) and (c), three spectra were measured on different areas for each sample. All the spectra were measured without a convergent lens. (d) Schematics of the two-photon excited fluorescence process in fluorescence emitter-doped TADF DA exciplex.

To study the influence of FRET on TPEF, TPEF properties of DA blends with and without fluorescent dopants were investigated under the same conditions. We found that the intensities of TPEF are immensely increased after doping 2% TTPA and 2% DCM. We note that TPEF intensities of DA blends doped with fluorescent emitters exceed the full scale, like measuring with a convergent lens. Therefore, all the long-wavelength-excited fluorescence spectra of TTPA- and DCM-doped blends were measured without a convergent lens in this work. Under this condition, the intensities of undoped DA blend are too weak to be detected [Figs. 6(b) and 6(c)]. The PLQYs of TTPA- and DCM-doped DA blends also confirm the enhancement of fluorescence. After doping with 2% TTPA and DCM, PLQYs of 98.65% and 20.86% were measured, respectively. These values are greatly increased compared to that of an undoped DA blend, indicating the existence of a FRET-related one- and two-photon fluorescence enhancement mechanism in a fluorescent emitter-doped DA blend. As shown in Fig. 6(d), the rapid FRET process from the singlet state ^{1}EX of the DA exciplex host to the singlet ^{1}EM state of the fluorescent emitter reduces the loops between ^{1}EX and ^{3}EX and thus the nonradiative energy loss during the waiting period for RISC, leading to an extremely high PLQY of FRET-type TADF blends and immensely enhanced TPEF intensities [60]. We note that there is also an energy loss mechanism; namely, the Dexter energy transfer (DET) process from the triplet state ^{3}EX of the DA exciplex host to the triplet ^{3}EM state of the fluorescent emitter [26]. Unlike the long-range FRET process, DET is a short-range process that is remarkable only in those blends with high dopant concentrations [61,62]. We also note that the observed enhancement of TPEF is larger than the values of the corresponding PLQY. This indicates that there may exist an additional possible enhancement mechanism for TPEF. Because the PLQY of TTPA-doped DA blend is up to 98.65% and there is not much room to improve, we speculate that the additional fluorescence is coming from the TPA process. Besides the TPA by D or A components, the intermolecular CT interaction in the excited states of exciplex may also facilitate the two-photon absorption.

4. CONCLUSION

In conclusion, we studied upconversion fluorescence in thin films based on an electron DA exciplex of TAPC:3TPYMB (1:1) and blends doped with 2% TTPA or 2% DCM fluorescent emitters. It is found that the color-adjustable upconversion fluorescence could be immensely enhanced in a fluorescent emitter-doped TADF DA exciplex. The RISC processes from ^{3}EX to ^{1}EX and consequently the rapid FRET process from ^{1}EX of the DA exciplex host to the singlet ^{1}EM state of the fluorescent emitter reduce the nonradiative energy loss and lead to immensely enhanced TPEF intensities.

By analyzing the relationship between the TPEF enhancements and the PLQYs in a series of samples, we also identified a new TPA gain mechanism related to the intermolecular CT interaction in the TADF DA exciplex system. We believe our findings may provide a new avenue for a material design strategy for highly efficient TPEF materials.

Funding. National Natural Science Foundation of China (11874237); Natural Science Foundation of Shandong Province (ZR2018MF030); Major Program of Shandong Province Natural Science Foundation (ZR2019ZD43).

Disclosures. The authors declare no conflicts of interest.

REFERENCES

1. K. Li, Z. Zhu, P. Cai, R. Liu, N. Tomczak, D. Ding, J. Liu, W. Qin, Z. Zhao, Y. Hu, X. Chen, B. Z. Tang, and B. Liu, "Organic dots with aggregation-induced emission (AIE dots) characteristics for dual-color cell tracing," Chem. Mater. **25**, 4181–4187 (2013).
2. L. M. Baugh, Z. Liu, K. P. Quinn, S. Osseiran, C. L. Evans, G. S. Huggins, P. W. Hinds, L. D. Black, and I. Georgakoudi, "Nondestructive two-photon excited fluorescence imaging identifies early nodules in calcific aortic-valve disease," Nat. Biomed. Eng. **1**, 914–924 (2017).
3. Y. Tang, Y. Li, X. Hu, H. Zhao, Y. Ji, L. Chen, W. Hu, W. Zhang, X. Li, X. Lu, W. Huang, and Q. Fan, ""Dual lock-and-key"-controlled nanoprobes for ultrahigh specific fluorescence imaging in the second near-infrared window," Adv. Mater. **30**, 1801140 (2018).
4. F. Terenziani, C. Katan, E. Badaeva, S. Tretiak, and M. Blanchard-Desce, "Enhanced two-photon absorption of organic chromophores: theoretical and experimental assessments," Adv. Mater. **20**, 4641–4678 (2008).
5. M. Drobizhev, N. S. Makarov, S. E. Tillo, T. E. Hughes, and A. Rebane, "Two-photon absorption properties of fluorescent proteins," Nat. Methods **8**, 393–399 (2011).
6. H. M. Kim and B. R. Cho, "Small-molecule two-photon probes for bioimaging applications," Chem. Rev. **115**, 5014–5055 (2015).
7. M. Rumi, J. E. Ehrlich, A. A. Heikal, J. W. Perry, S. Barlow, Z. Y. Hu, D. Mccordmaughon, T. C. Parker, H. Rockel, and S. Thayumanavan, "Structure-property relationships for two-photon absorbing chromophores: Bis-donor diphenylpolyene and bis (styryl) benzene derivatives," J. Am. Chem. Soc. **122**, 9500–9510 (2000).
8. G. S. He, L. Tan, Q. Zheng, and P. N. Prasad, "Multiphoton absorbing materials: molecular designs, characterizations, and applications," Chem. Rev. **108**, 1245–1330 (2008).
9. K. H. Myung and C. B. Rae, "Two-photon materials with large two-photon cross sections. Structure-property relationship," Chem. Commun. **2**, 153–164 (2009).
10. Z. R. Grabowski, K. Rotkiewicz, and W. Rettig, "Structural changes accompanying intramolecular electron transfer: focus on twisted intramolecular charge-transfer states and structures," Chem. Rev. **103**, 3899–4031 (2003).
11. Y. Li, T. Liu, H. Liu, M. Z. Tian, and Y. Li, "Self-assembly of intramolecular charge-transfer compounds into functional molecular systems," Acc. Chem. Res. **47**, 1186–1198 (2014).
12. M. Pawlicki, H. A. Collins, R. G. Denning, and H. L. Anderson, "Two-photon absorption and the design of two-photon dyes," Angew. Chem. Int. Ed. Engl. **48**, 3244–3266 (2009).
13. C.-L. Sun, J. Li, X.-Z. Wang, R. Shen, S. Liu, J.-Q. Jiang, T. Li, Q.-W. Song, Q. Liao, H.-B. Fu, J.-N. Yao, and H.-L. Zhang, "Rational design of organic probes for turn-on two-photon excited fluorescence imaging and photodynamic therapy," Chem **5**, 600–616 (2019).
14. A. Cesaretti, P. Foggi, C. G. Fortuna, F. Elisei, A. Spalletti, and B. Carlotti, "Uncovering structure–property relationships in push–pull chromophores: a promising route to large hyperpolarizability and two-photon absorption," J. Phys. Chem. C **124**, 15739–15748 (2020).
15. H. Tanaka, K. Shizu, H. Miyazaki, and C. Adachi, "Efficient green thermally activated delayed fluorescence (TADF) from a phenoxazine-triphenyltriazine (PXZ-TRZ) derivative," Chem. Commun. **48**, 11392–11394 (2012).
16. L. Xu and Q. Zhang, "Recent progress on intramolecular charge-transfer compounds as photoelectric active materials," Sci. China Mater. **60**, 1093–1101 (2017).
17. A. Endo, K. Sato, K. Yoshimura, T. Kai, A. Kawada, H. Miyazaki, and C. Adachi, "Efficient up-conversion of triplet excitons into a singlet state and its application for organic light emitting diodes," Appl. Phys. Lett. **98**, 083302 (2011).
18. K. Goushi, K. Yoshida, K. Sato, and C. Adachi, "Organic light-emitting diodes employing efficient reverse intersystem crossing for triplet-to-singlet state conversion," Nat. Photonics **6**, 253–258 (2012).
19. H. Uoyama, K. Goushi, K. Shizu, H. Nomura, and C. Adachi, "Highly efficient organic light-emitting diodes from delayed fluorescence," Nature **492**, 234–238 (2012).
20. K. Goushi and C. Adachi, "Efficient organic light-emitting diodes through up-conversion from triplet to singlet excited states of exciplexes," Appl. Phys. Lett. **101**, 023306 (2012).
21. P. B. Deotare, W. Chang, E. Hontz, D. N. Congreve, L. Shi, P. D. Reusswig, B. Modtland, M. E. Bahlke, C. K. Lee, A. P. Willard, V. Bulovic, T. Van Voorhis, and M. A. Baldo, "Nanoscale transport of charge-transfer states in organic donor-acceptor blends," Nat. Mater. **14**, 1130–1134 (2015).
22. W. Liu, J.-X. Chen, C.-J. Zheng, K. Wang, D.-Y. Chen, F. Li, Y.-P. Dong, C.-S. Lee, X.-M. Ou, and X.-H. Zhang, "Novel strategy to develop exciplex emitters for high-performance OLEDs by employing thermally activated delayed fluorescence materials," Adv. Funct. Mater. **26**, 2002–2008 (2016).
23. K.-H. Kim, C.-K. Moon, J. W. Sun, B. Sim, and J.-J. Kim, "Triplet harvesting by a conventional fluorescent emitter using reverse intersystem crossing of host triplet exciplex," Adv. Opt. Mater. **3**, 895–899 (2015).
24. X. K. Liu, Z. Chen, C. J. Zheng, M. Chen, W. Liu, X. H. Zhang, and C. S. Lee, "Nearly 100% triplet harvesting in conventional fluorescent dopant-based organic light-emitting devices through energy transfer from exciplex," Adv. Mater. **27**, 2025–2030 (2015).
25. H. Nakanotani, T. Higuchi, T. Furukawa, K. Masui, K. Morimoto, M. Numata, H. Tanaka, Y. Sagara, T. Yasuda, and C. Adachi, "High-efficiency organic light-emitting diodes with fluorescent emitters," Nat. Commun. **5**, 4016 (2014).
26. Q. Wang, Q.-S. Tian, Y.-L. Zhang, X. Tang, and L.-S. Liao, "High-efficiency organic light-emitting diodes with exciplex hosts," J. Mater. Chem. C **7**, 11329–11360 (2019).
27. J. Kalinowski, G. Giro, M. Cocchi, V. Fattori, and P. Di Marco, "Unusual disparity in electroluminescence and photoluminescence spectra of vacuum-evaporated films of 1,1-bis((di-4-tolylamino) phenyl) cyclohexane," Appl. Phys. Lett. **76**, 2352–2354 (2000).
28. H. J. Lee, J. Sohn, J. Hwang, S. Y. Park, C. Haeyoung, and M. Cha, "Triphenylamine-cored bifunctional organic molecules for two-photon absorption and photorefraction," Chem. Mater. **16**, 456–465 (2004).
29. C. D. Entwistle and T. B. Marder, "Applications of three-coordinate organoboron compounds and polymers in optoelectronics," Chem. Mater. **16**, 4574–4585 (2004).
30. D. Tanaka, T. Takeda, T. Chiba, S. Watanabe, and J. Kido, "Novel electron-transport material containing boron atom with a high triplet excited energy level," Chem. Lett. **36**, 262–263 (2007).
31. D. X. Cao, Z. Q. Liu, Q. Fang, G. B. Xu, G. Xue, G. Q. Liu, and W. T. Yu, "Blue two-photon excited fluorescence of several D-π-D, A-π-A, and D-π-A compounds featuring dimesitylboryl acceptor," J. Organomet. Chem. **689**, 2201–2206 (2004).
32. R. Kannan, G. S. He, J. T. Lin, P. N. Prasad, R. A. V. And, and L. Tan, "Toward highly active two-photon absorbing liquids. synthesis and characterization of 1,3,5-triazine-based octupolar molecules," Chem. Mater. **16**, 185–194 (2004).
33. Z. Liu, Q. Fang, D. Cao, D. Wang, and G. Xu, "Triaryl boron-based A-π-A vs triaryl nitrogen-based D-π-D quadrupolar compounds for single- and two-photon excited fluorescence," Org. Lett. **6**, 2933–2936 (2004).

34. Y. Seino, H. Sasabe, Y. J. Pu, and J. Kido, "High-performance blue phosphorescent OLEDs using energy transfer from exciplex," Adv. Mater. **26**, 1612–1616 (2014).
35. N. Bunzmann, S. Weissenseel, L. Kudriashova, J. Gruene, B. Krugmann, J. V. Grazulevicius, A. Sperlich, and V. Dyakonov, "Optically and electrically excited intermediate electronic states in donor: acceptor based OLEDs," Mater. Horiz. **7**, 1126–1137 (2020).
36. M. Regnat, K. P. Pernstich, K. H. Kim, J. J. Kim, F. Nüesch, and B. Ruhstaller, "Routes for efficiency enhancement in fluorescent TADF exciplex host OLEDs gained from an electro-optical device model," Adv. Electron. Mater. **6**, 1900804 (2020).
37. H. A. Al Attar and A. P. Monkman, "Electric field induce blue shift and intensity enhancement in 2D exciplex organic light emitting diodes; controlling electron-hole separation," Adv. Mater. **28**, 8014–8020 (2016).
38. D. Graves, V. Jankus, F. B. Dias, and A. Monkman, "Photophysical investigation of the thermally activated delayed emission from films of m-MTDATA:PBD exciplex," Adv. Funct. Mater. **24**, 2343–2351 (2014).
39. Q. Huang, S. Zhao, P. Wang, Z. Qin, Z. Xu, D. Song, B. Qiao, and X. Xu, "Investigating the evolution of exciplex states in thermally activated delayed fluorescence organic light-emitting diodes by transient measurement," J. Lumin. **201**, 38–43 (2018).
40. D. Rehm and A. Weller, "Kinetics of fluorescence quenching by electron and H-atom transfer," Isr. J. Chem. **8**, 259–271 (1970).
41. B. Dereka, M. Koch, and E. Vauthey, "Looking at photoinduced charge transfer processes in the IR: answers to several long-standing questions," Acc. Chem. Res. **50**, 426–434 (2017).
42. D. J. Stewart, M. J. Dalton, R. N. Swiger, T. M. Cooper, J. E. Haley, and L. S. Tan, "Exciplex formation in blended spin-cast films of fluorene-linked dyes and bisphthalimide quenchers," J. Phys. Chem. A **117**, 3909–3917 (2013).
43. M. Zhang, W. Liu, C. J. Zheng, K. Wang, Y. Z. Shi, X. Li, H. Lin, S. L. Tao, and X. H. Zhang, "Tricomponent exciplex emitter realizing over 20% external quantum efficiency in organic light-emitting diode with multiple reverse intersystem crossing channels," Adv. Sci. **6**, 1801938 (2019).
44. W. Zhu, R. Zheng, X. Fu, H. Fu, Q. Shi, Y. Zhen, H. Dong, and W. Hu, "Revealing the charge-transfer interactions in self-assembled organic cocrystals: two-dimensional photonic applications," Angew. Chem. Int. Ed. Engl. **54**, 6785–6789 (2015).
45. L. Sun, W. Zhu, W. Wang, F. Yang, C. Zhang, S. Wang, X. Zhang, R. Li, H. Dong, and W. Hu, "Intermolecular charge-transfer interactions facilitate two-photon absorption in styrylpyridine-tetracyanobenzene cocrystals," Angew. Chem. Int. Ed. Engl. **56**, 7831–7835 (2017).
46. D. Chen, Z. Wang, D. Wang, Y.-C. Wu, C.-C. Lo, A. Lien, Y. Cao, and S.-J. Su, "Efficient exciplex organic light-emitting diodes with a bipolar acceptor," Org. Electron. **25**, 79–84 (2015).
47. K.-H. Kim, S.-J. Yoo, and J.-J. Kim, "Boosting triplet harvest by reducing nonradiative transition of exciplex toward fluorescent organic light-emitting diodes with 100% internal quantum efficiency," Chem. Mater. **28**, 1936–1941 (2016).
48. P. L. dos Santos, F. B. Dias, and A. P. Monkman, "Investigation of the mechanisms giving rise to TADF in exciplex states," J. Phys. Chem. C **120**, 18259–18267 (2016).
49. M. Sarma and K. T. Wong, "Exciplex: an intermolecular charge-transfer approach for TADF," ACS Appl. Mater. Interfaces **10**, 19279–19304 (2018).
50. W. Hu, L. Guo, L. Bai, X. Miao, Y. Ni, Q. Wang, H. Zhao, M. Xie, L. Li, X. Lu, W. Huang, and Q. Fan, "Maximizing aggregation of organic fluorophores to prolong fluorescence lifetime for two-photon fluorescence lifetime imaging," Adv. Healthcare Mater. **7**, 1800299 (2018).
51. V. Jankus, P. Data, D. Graves, C. McGuinness, J. Santos, M. R. Bryce, F. B. Dias, and A. P. Monkman, "Highly efficient TADF OLEDs: how the emitter-host interaction controls both the excited state species and electrical properties of the devices to achieve near 100% triplet harvesting and high efficiency," Adv. Funct. Mater. **24**, 6178–6186 (2014).
52. C. Dai, Z. Wei, Z. Chen, X. Liu, J. Fan, J. Zhao, C. Zhang, Z. Pang, and S. Han, "Efficient two-photon excited fluorescence from charge-transfer cocrystals based on centrosymmetric molecules," Adv. Opt. Mater. **7**, 1900838 (2019).
53. H. Nakanotani, T. Furukawa, K. Morimoto, and C. Adachi, "Long-range coupling of electron-hole pairs in spatially separated organic donor-acceptor layers," Sci. Adv. **2**, e1501470 (2016).
54. T. Higuchi, H. Nakanotani, and C. Adachi, "High-efficiency white organic light-emitting diodes based on a blue thermally activated delayed fluorescent emitter combined with green and red fluorescent emitters," Adv. Mater. **27**, 2019–2023 (2015).
55. Z. Pang, D. Sun, C. Zhang, S. Baniya, O. Kwon, and Z. V. Vardeny, "Manipulation of emission colors based on intrinsic and extrinsic magneto-electroluminescence from exciplex organic light-emitting diodes," ACS Photon. **4**, 1899–1905 (2017).
56. Y. C. Lo, T. H. Yeh, C. K. Wang, B. J. Peng, J. L. Hsieh, C. C. Lee, S. W. Liu, and K. T. Wong, "High-efficiency red and near-infrared organic light-emitting diodes enabled by pure organic fluorescent emitters and an exciplex-forming cohost," ACS Appl. Mater. Interfaces **11**, 23417–23427 (2019).
57. M. Wu, Z. Wang, Y. Liu, Y. Qi, and J. Yu, "Non-doped phosphorescent organic light-emitting devices with an exciplex forming planar structure for efficiency enhancement," Dyes Pigm. **164**, 119–125 (2019).
58. F. Gao, Q. Liao, Z. Z. Xu, Y. H. Yue, Q. Wang, H. L. Zhang, and H. B. Fu, "Strong two-photon excited fluorescence and stimulated emission from an organic single crystal of an oligo(phenylene vinylene)," Angew. Chem. Int. Ed. Engl. **49**, 732–735 (2010).
59. T. He, Z. B. Lim, L. Ma, H. Li, D. Rajwar, Y. Ying, Z. Di, A. C. Grimsdale, and H. Sun, "Large two-photon absorption of terpyridine-based quadrupolar derivatives: towards their applications in optical limiting and biological imaging," Chem. Asian J. **8**, 564–571 (2013).
60. P. Xiao, J. Huang, Y. Yu, J. Yuan, D. Luo, B. Liu, and D. Liang, "Recent advances of exciplex-based white organic light-emitting diodes," Appl. Sci. **8**, 1449 (2018).
61. X. Song, D. Zhang, H. Li, M. Cai, T. Huang, and L. Duan, "Exciplex system with increased donor-acceptor distance as the sensitizing host for conventional fluorescent OLEDs with high efficiency and extremely low roll-off," ACS Appl. Mater. Interfaces **11**, 22595–22602 (2019).
62. C. Zhang, Y. S. Zhao, and J. Yao, "Organic composite nanomaterials: energy transfers and tunable luminescent behaviors," New J. Chem. **35**, 973–978 (2011).